Scientific Research Publishing

Geomaterials, 2026, 16(1), 34-51
https://www.scirp.org/journal/gm
ISSN Online: 2161-7546
ISSN Print: 2161-7538

Statistical Modeling of Geotechnical Parameters of a Shallow Foundation Located in Daral Peulh (Thiès, Senegal)

Hamed Fall, Déthié Sarr, Arthur Omar Mendy, Samba Magat Gaye

Département de Géotechnique, UFR Sciences de l'Ingénieur, Université Iba Der Thiam de Thiès, Thiès, Senegal
Email: hamed.fall@univ-thie.sn

How to cite this paper: Fall, H., Sarr, D., Mendy, A.O. and Gaye, S.M. (2026) Statistical Modeling of Geotechnical Parameters of a Shallow Foundation Located in Daral Peulh (Thiès, Senegal). *Geomaterials*, **16**, 34-51.
https://doi.org/10.4236/gm.2026.161003

Received: December 1, 2025
Accepted: January 18, 2026
Published: January 21, 2026

Abstract

In general, the analysis and design of civil engineering structures are based on deterministic approaches where uncertainties in various parameters (soil characteristics, loading, etc.) are not taken into account. In recent decades, the description and analysis of uncertainty in geotechnical engineering, with a focus on the safety of structures, have become increasingly important issues. To fix the level of risk for which geotechnical parameter values must be determined, the Eurocodes have introduced an approach based on the statistical processing of soil data. This paper presents the statistical modeling of geotechnical parameters (cohesion, friction angle, specific weight) of a shallow foundation soil from Daral Peulh area located in Thies in Senegal. Laboratory tests for soil identification were conducted on 26 samples. After outliers, values determined and treated with boxplot method, graphical methods and Kolmogorov and Shapiro-Wilk tests were used to determine the probability distributions associated with geotechnical parameters and the bearing capacity of a shallow foundation. The results conclude after outliers treatment with 5% risk, the probability distributions of the cohesion, the friction angle and the specific weight are normal distributions and can be used for probability design. However, the variability around their means is high for the cohesion, the friction angle and the bearing capacity. For the bearing, the most suitable probability distribution in this case is the lognormal distribution.

Keywords

Statistical Modeling, Uncertainty, Kolmogorov-Smirnov, Terzaghi, Shallow Foundation, Eurocodes, Shapiro-Wilk

1. Introduction

Traditionally, the analysis and dimensioning of geotechnical structures are based on deterministic approaches. The hazards and uncertainties of the various parameters (soil characteristics, loading, etc.) are taken into account in a simplified manner in the form of an overall safety factor [1]. To take into account the hazards and uncertainties inherent in parameters, reliability theory is currently being used more and more in geotechnical engineering. This has been made possible by significant advances in quantifying uncertainties in soil parameters. Indeed, the high variability of geotechnical parameters, their changing nature over time and space, and the significant uncertainty that affects them, make it necessary to consider them in the form of random fields. The probabilistic approach addresses problems in a completely different way, by postulating a priori the random nature of the quantities involved in the phenomena studied and in the behavior models used to describe these phenomena [2]. The application of statistics and probability in the field of geotechnical engineering began at the Central Laboratory for Bridges and Roads (LCPC), where initial research was conducted on certain types of soil. Previous studies have provided a practical alternative for applying probabilistic design methods to structures and even statistical analysis of geotechnical data from a given site, which has led to greater pessimism about the practical usefulness of this type of research ([3] [4]). To help for probabilistic design of a shallow foundation, this paper shows a statistical analysis for a soil located in Daral Peulh in Thiès area in Senegal. The study is done with 26 samples taken at two points close to each other. After a laboratory test for determining the geotechnical parameters (cohesion, friction angle, specific weight), the bearing capacity is calculated, and the statistical indicators and outliers are determined for all parameters. According to the boxplot method, all parameters were treated and with 5% risk, a Kolmogorov-Smirnov and Shapiro-Wilk tests were realized with RStudio software to determine their probability distributions, also using graphical hypothesis testing.

2. Methods and Materials

2.1. Statistical Modeling of Soil Geotechnical Parameters

The statistical analysis approach to geotechnical data is based on summarizing a parameter with a best estimate using the mean and a measure of uncertainty using the standard deviation (or variance) [5]. These different uncertainties affect engineering calculations and must be analyzed and combined to construct a statistical soil profile, which provides a better description of the soil. Statistical modeling of the geotechnical parameters of a soil involves the use of statistical techniques to analyze geotechnical data and model soil properties. This modeling can help geotechnical engineers understand soil characteristics, predict its behavior, and design appropriate structures and foundations. Soil properties are usually scattered. Graphs and mathematical techniques are useful for summarizing this dispersion, thereby facilitating a better understanding of the data. The

graphical representations presented in the previous section only allow for a visual analysis of the data distribution. It is therefore necessary to have statistical indicators [6] [7].

2.2. Statistical Indicators

Graphs and mathematical techniques are used to obtain a better estimate of soil properties on the one hand, and a quantitative assessment of the uncertainty of this estimate on the other. After collecting data on site and conducting laboratory tests, the first step is to plot histograms. Then, for better application in engineering, a mathematical description based on the mean and standard deviation is made. The mean and standard deviation summarize important information about the measured parameter and provide a useful description of the dispersion of the data for their use [8].

Consider a set n of data $\{x_1, \cdots, x_n\}$, the arithmetic mean $\overline{x}$ is given by the Equation (1)

$$\overline{x} = (1/n)\sum_{i=1}^{n} x_i \tag{1}$$

The median Q_2 (second quartile) can be associated with the mean. The median is the value that divides the data into two equal parts. In other words, 50% of the values are below the median and 50% are above it. We may also need more information, such as:

- The lower quartile Q_1 is the value for which 25% of the values are lower than Q1 and 75% are higher than it.

- The upper quartile Q_3 is the value for which 75% of the values are less than Q3 and 25% are greater than it.

The variance V is given by Equation (2):

$$V = (1/n)\sum_{i=1}^{n} (x_i - \overline{x})^2 \tag{2}$$

The standard deviation σ_x, which is a measure of dispersion, will be calculated using Equation (3). The standard deviation is also useful when comparing the dispersion of two separate data sets that have approximately the same mean.

$$\sigma_x = \sqrt{(1/n)\sum_{i=1}^{n} (x_i - \overline{x})^2} \tag{3}$$

For a mean $\overline{x}$ and a standard deviation σ_x.

- approximately 68% of the data is mainly within the range $]\overline{x} - \sigma_x; \overline{x} + \sigma_x[$.

- approximately 95% of the data is essentially within the range $]\overline{x} - 2\sigma_x; \overline{x} + 2\sigma_x[$.

- approximately 99% of the data is essentially within the range $]\overline{x} - 3\sigma_x; \overline{x} + 3\sigma_x[$

thus the coefficient of variation C_v which is dimensionless, is given by Equation (4).

$$C_v = \overline{x}/\sigma_x \tag{4}$$

It allows us to consider that the sample has significant variability if $C_v > 0.15$. The data show little variability if $C_v \leq 0.15$ and we consider that the empirical mean alone is a good summary of the entire sample.

2.3. Goodness-of-Fit Tests

A goodness-of-fit test is used to demonstrate whether data from a sample follows a probability distribution. Thus, when performing geotechnical design using software that employs probabilistic methods, it is possible to characterize geotechnical parameters using probability distributions that have been verified by goodness-of-fit tests. There are many tests to verify whether or not a sample follows a given probability distribution; this type of test is called a goodness-of-fit test [9] [10].

2.3.1. Graphical Methods

In this paper, we use the following four (4) methods

- Distribution Function Method
- Histogram Method
- Q-Q Plot Method
- Boxplot Method

2.3.2. Kolmogorov-Smirnov Test

Consider a sample of size n $\{x_1,\cdots,x_n\}$ from a random variable X. Let $F_n(x)$ be the empirical distribution function associated with the data and $F_{th}(x)$ be the distribution function associated with a given distribution L.

We consider the following assumptions:

H_0: X follows the law of L H_1; X does not follow the law of L.

The idea behind Kolmogorov's test is to verify the hypothesis. H_0 with a risk α. More $F_n(x)$ differs from $F_{th}(x)$, more the rejection of H_0 is significant.

This consists of finding the maximum difference D defined by Equations (5) and (6)

$$D=\max_{x\in[1,n]}\left|F_n(x)-F_{th}(x)\right| \tag{5}$$

$$D=\max_{x\in[1,n]}\left(\left|F_{th}(x)-(i-1)/n\right|,\left|i/n-F_{th}(x)\right|\right) \tag{6}$$

with $F_n(x)$ defined par:

- $F_n(x)=0$ si $x<x_1$.
- $F_n(x)=i/n$ si $x_{i-1}<x<x_i$.
- $F_n(x)=1$ si $t>x_n$.

Read the value of D_α for a given risk α from Kolmogorov's table [10]. If $D>D_\alpha$, therefore, the null hypothesis H_0 is accepted; otherwise, it is rejected. Alternatively, by calculating p-value $=P(D>D_\alpha)$. If $p>\alpha$, the hypothesis H_0 is accepted.

3. Results and Discussions

3.1 Area Study Presentation

The soil samples used in this study were taken from the Daral Peulh site in the Thiès region in two areas named E1 and E2 as shown in **Figure 1**.

To conduct laboratory tests, soil a total of 26 samples were taken at several points in zone E1 (13 points) and zone E2 (13 points) as shown in **Figure 1** at varying

depths (between 0.5 m and 1 m) and coordinates in the following Table 1.

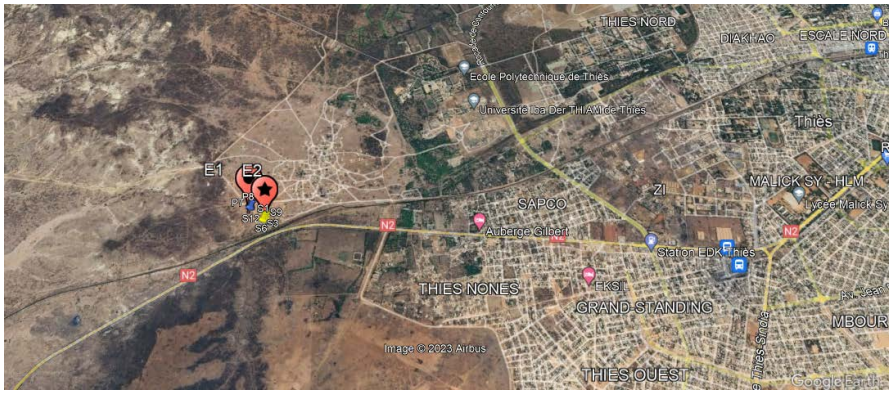

Figure 1. Localisation du site et les points de prélèvements (Google Earth Pro, 2015).

Table 1. Sampling point coordinates.

Points	Latitude	Longitude
E1P0	14˚47'7.79"N	16˚58'45.89"O
E1P1	14˚47'4.08"N	16˚58'42.04"O
E1P2	14˚47'4.2"N	16˚58'41.80"O
E1P3	14˚47'4.07"N	16˚58'41.80"O
E1P4	14˚47'4.02"N	16˚58'42.52"O
E1P5	14˚47'4.16"N	16˚58'42.33"O
E1P6	14˚47'4.61"N	16˚58'42.62"O
E1P7	14˚47'4.33"N	16˚58'42.61"O
E1P8	14˚47'4.52"N	16˚58'42.38"O
E1P9	14˚47'4.66"N	16˚58'42.12"O
E1P10	14˚47'4.70"N	16˚58'41.71"O
E1P11	14˚47'4.55"N	16˚58'41.90"O
E1P12	14˚47'4.32"N	16˚58'42.07"O
E2P0	14˚47'4.40"N	16˚58'41.60"O
E2P1	14˚47'7.82"N	16˚58'46.30"O
E2P2	14˚47'7.97"N	16˚58'46.30"O
E2P3	14˚47'7.98"N	16˚58'45.91"O
E2P4	14˚47'7.98"N	16˚58'46.08"O
E2P5	14˚47'7.78"N	16˚58'46.06"O
E2P6	14˚47'7.63"N	16˚58'45.86"O

Continued

E2P7	14˚47'7.60"N	16˚58'46.02"O
E2P8	14˚47'7.60"N	16˚58'46.21"O
E2P9	14˚47'7.69"N	16˚58'46.28"O
E2P10	14˚47'7.87"N	16˚58'46.16"O
E2P11	14˚47'7.72"N	16˚58'45.94"O
E2P12	14˚47'7.74"N	16˚58'46.17"O

3.2. Soil Identification Test

3.2.1. Granulometry Analysis and Atterberg Limits

The granulometry analysis, which consists of determining the granularity of the soil, is carried out in accordance with standard NF P 94-056. This involves taking a 5 kg sample of the material, placing it in an oven, then washing it through an 80 mm sieve until the water runs clear. This washed material is then returned to the oven for 24 hours to dry. Finally, it is sieved using sieves ranging from 50 mm to 0.08 mm, which corresponds to sieve modules from 48 to 20 according to AFNOR. At the end of each sieving stage, the cumulative weight of the rejects is weighed. Figure 2(a) and Figure 2(b) show the sieving and weighing during the granulometric test.

(a) Sieving

(b) Weighing

Figure 2. Sieving and weighing for particle size analysis.

The particle size analysis curves for samples E1P0 and E2P0 are shown in Figure 3 and Figure 4.

Table 2 summarizes the results of the particle size analysis. The liquidity limits of samples E1P0 and E2P0 corresponding to the 25th impacts were determined and are 25.5% and 24.4%, respectively. The plasticity limits are 15.6% and 9.9%, respectively. Thus, based on the LCP classification, samples E1P0 and E2P1 can be described as clayey lateritic gravels with low plasticity.

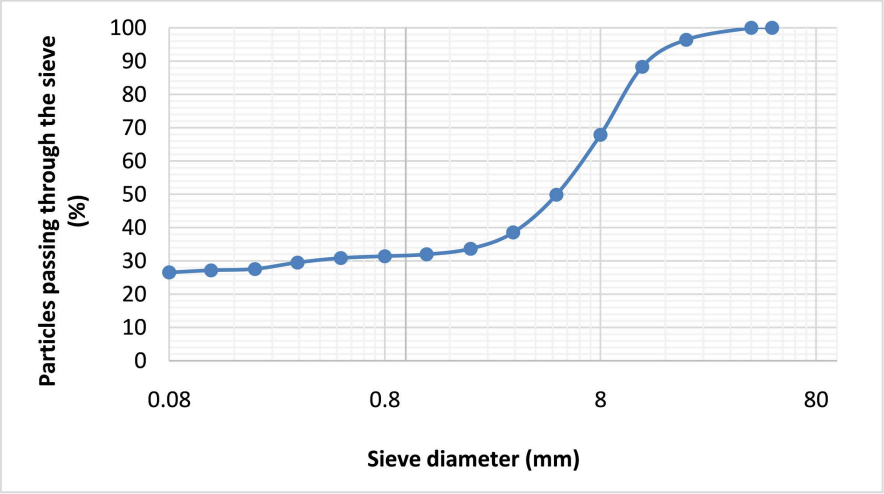

Figure 3. Granulometry curve of E1P0 sampling.

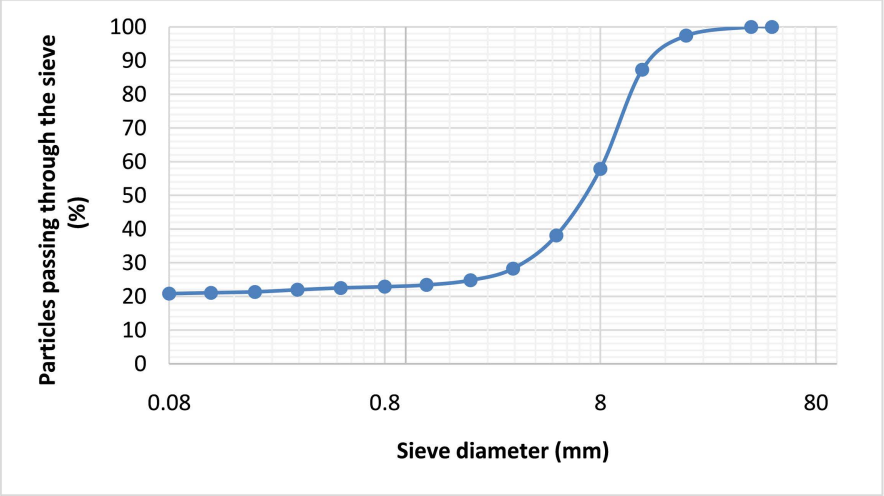

Figure 4. Granulometric curve of E2P0 sampling.

Table 2. Particle size analysis.

Sample	Granulometric Analysis							Atterberg limits		
	Sieve		Diameter (mm)			Coefficients				
	2 mm % (*R*)	0.08 mm % (*P*)	D_{10}	D_{30}	D_{60}	C_u	C_c	W_L (%)	W_P (%)	I_P (%)
Area E1P0	66.32	31.42	0.018	0.31	6.8	377.78	0.76	25.5	15.6	9.9
Area E2P0	75.16	22.92	0.011	3.5	8.5	772.73	131.02	24.4	9.9	14.5

(*R*): Retained (*P*): Passing; W_L the liquidity limit (which separates the plastic state from the liquid state); W_P the plasticity limit (which separates the plastic state from the solid state); I_P soil plasticity index.

3.2.2. Physical and Mechanical Tests

The specific weight γ of soil solids is determined in accordance with standard

NF P 94-054. Table 3 shows the results obtained for all sampling points presented in Table 1.

Table 3. Specific gravity of all samples.

(a) zone E1	
Points	Specific gravity γ_s (kN/m^3)
E1P0	25.74
E1P1	26
E1P2	25.85
E1P3	25.77
E1P4	25.82
E1P5	25.75
E1P6	24.01
E1P7	23.93
E1P8	23.64
E1P9	23.62
E1P10	24.24
E1P11	24.33
E1P12	26.28
(b) zone E2	
Points	Specific gravity γ_s (kN/m^3)
E2P0	25.94
E2P1	24.7
E2P2	25.62
E2P3	25.55
E2P	24.28
E2P5	23.3
E2P6	25.99
E2P7	24.62
E2P8	26.36
E2P9	24.48
E2P10	23.35
E2P11	22.83
E2P12	25.76

Based on the results in the table above, the bulk densities of the solid grains in samples E1 and E2 are obtained and are 25.74 kN/m³ and 25.94 kN/m³ respectively.

The direct shear test according to NF P94-071 made it possible to evaluate the resistance by determining the cohesion (C) and the angle of friction (φ) (Table 4).

Table 4. Shear tests of all samples.

Points	C (kPa)	φ (˚)
E1P0	94.24	20.63
E1P1	20.34	11.55
E1P2	44.76	6.94
E1P3	34.43	6.92
E1P4	22.58	9.98
E1P5	28.90	7.92
E1P6	18.03	9.98
E1P7	28.93	8.94
E1P8	23.75	9.24
E1P9	17.16	8.43
E1P10	31.79	8.88
E1P11	27.20	8.79
E1P12	10.12	8.85
E2P0	42.41	7.18
E2P1	20.004	6.93
E2P2	23.04	8.45
E2P3	18.10	7.07
E2P4	22.8	16.52
E2P5	30.36	14.89
E2P6	27.36	6.15
E2P7	22.17	7.67
E2P8	27.36	6.15
E2P9	29.97	22.2
E2P10	84.04	23.55
E2P11	20.65	9.39
E2P12	16.77	6.38

Based on the test results, the bearing capacity of a shallow foundation according to Terzaghi was calculated using Equation (7). The results are shown on Table 5. The application concerns isolated footings with a width $B = L = 1.5$ m and an anchorage depth $D = 0.5$ m.

$$Q_p = \frac{1}{2} S_\gamma \gamma B N_\gamma + S_q \gamma D N_q + S_c c N_c \quad (7)$$

S_γ, S_q, S_c are the shape coefficients of the base.

N_γ, N_q, N_c are the bearing capacity factors depending on φ.

C: Cohesion of soil.

φ : Angle of internal friction.

γ : unit weight of soil.

Table 5. Bearing capacity of all samples.

(a) zone E1	
Points	Bearing Capacity Q_p
E1P0	2152.5
E1P1	318.7
E1P2	467.8
E1P3	366.7
E1P4	303.8
E1P5	332.12
E1P6	248.28
E1P7	351.08
E1P8	294.15
E1P9	208.15
E1P10	382.74
E1P11	332.80
E1P12	149.4
(b) zone E2	
Points	Bearing Capacity Q_p
E2P0	444.9
E2P1	224.34
E2P2	271.46
E2P3	206.71
E2P4	497.4
E2P5	541.61

Continued

E2P6	280.43
E2P7	261.17
E2P8	280.81
E2P9	916.24
E2P10	2588.1
E2P11	259.13
E2P12	181.96

3.3. Statistical Treatment

3.3.1. Determination of Statistical Indicators

In this section, some statistical indicators mentioned in paragraph 2.2 will be determined for the cohesion, friction angle, the specific gravity, and bearing capacity before outliers treatment. The results are presented in Table 6. The dispersion is significant for all parameters except for the specific gravity due to the coefficient of variation is bigger than 0.15 for all those parameters.

Table 6. Statistical indicators with outliers.

	Cohesion (kPa)	Friction Angle φ (˚)	Specific gravity (kN/m^3)	Bearing Capacity Q_p (kPa)
Sample size	26	26	26	26
Minimum	10.12	6.15	22.83	149.39
Maximum	94.24	23.55	26.36	2588.09
Mean	30.28	10.37	24.91	494.71
Median	25.48	8.82	25.13	311.23
Mode	27.36	9.98	22.83a	149.39a
Standard deviation	19.00	4.98	1.07	575.88
CoV	0.63	0.48	0.04	1.16

CoV: Coefficient of variation.

3.3.2. Outliers Treatment

First, these outliers must be detected by plotting scatter plots for each parameter. These scatter plots are shown in Figure 5(a) to Figure 5(d). One can see that some values are outliers for cohesion, friction angle and the bearing capacity. But for the specific weight there is no outliers.

For the detection of outliers, the box-and-whiskers (BW) method is used (Figure 6). This method allows the determination of maximum (XA) and minimum (XB) thresholders and the detection of outliers and is also used to assess the symmetry of a distribution. As Sanou [10] noted, if it is symmetrical, it can be assumed that the distribution follows a normal distribution, because a normal distribution is symmetrical, but the reverse is not true.

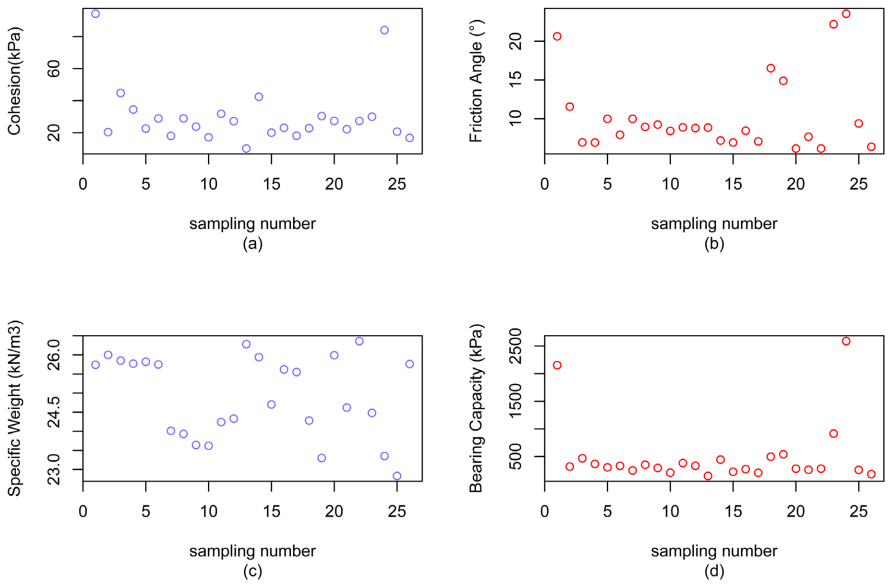

Figure 5. Scatter plot of all parameters.

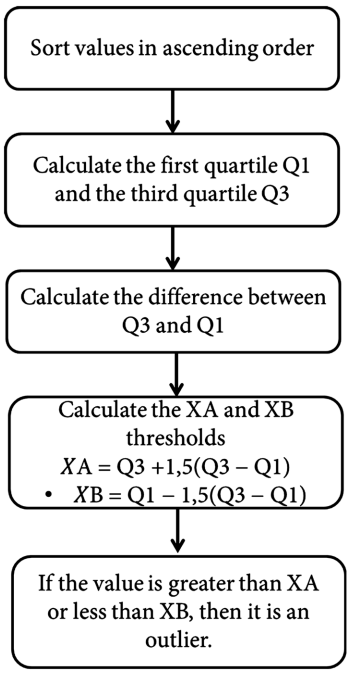

Figure 6. Outliers values detection with box-and-whiskers (BW).

Table 7 summarizes the outliers found. There are two outliers values for cohesion (84.04, 94.24), five outliers for friction angle (14.89, 16.52, 20.63, 22.20, 23.55), and three outliers values for bearing capacity (916.24, 2152.50, 2588.10). No outliers were detected for specific weight as mentioned before. It is important to pay particular attention to the transformation of variables when manipulating data, as this could cause outliers to appear. Also the conditions (for example measure error, sample error, etc.) in which the tests are carried out can cause the presence of outliers.

Table 7. Outliers detection.

Parameters	Sample size	Minimum	Maximum	XB	XA	Number of outliers
C (kPa)	26	10.120	94.240	5.65	45.03	2
φ (˚)	26	6.15	2.55	2.78	14.31	5
γ_s (kN/m^3)	26	22.83	26.36	21.234	28.584	No
Q_p (KPa)	26	149.388	2588.095	5.05	683.96	3

Using R-Studio software, the whisker plots (Figures 7(a)-(d)) show the positions of outliers for each parameter.

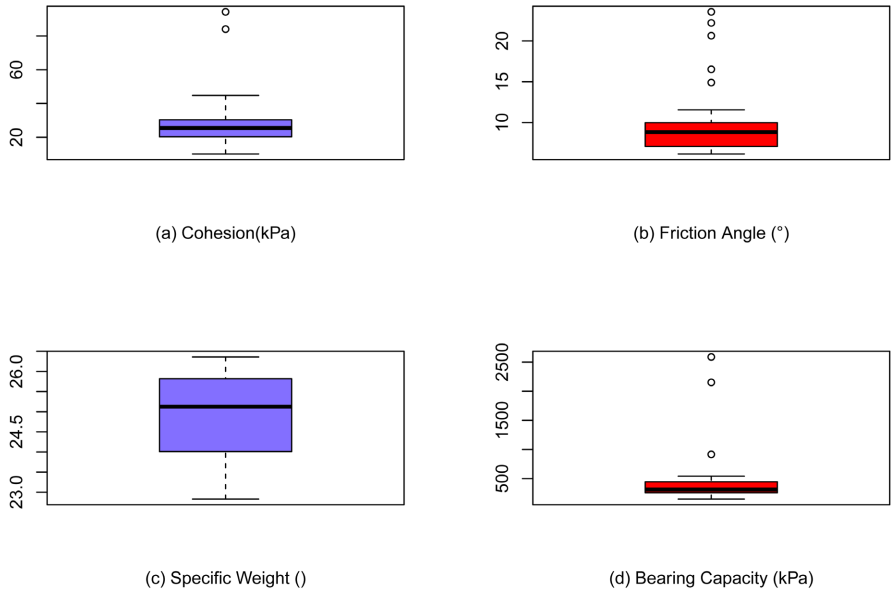

Figure 7. Boxplot for all parameters.

Next, one will present the case where values are processed using the box-whisker plot method. Figure 8 and Figure 9 show the histograms of cohesion, friction angle, and bearing capacity for the three cases (all values, with outliers treated, and with outliers removed), respectively. It seems that the probability distributions of the cohesion and the bearing capacity can be considered as Gaussian distributions but for the other parameters cannot conclude.

Table 8 shows the statistical indicators without outliers (outliers are treated). Except for the specific gravity, the coefficient of variation of all parameters is bigger than 0.15 that's mean a high variability around their mean for these parameters (cohesion, friction angle, bearing capacity).

3.3.3. Goodness Test

In this section of the paper, the graphical goodness-of-fit tests on the one hand and the Kolmogorov-Smirnov and Shapiro-Wilk tests on the other hand will be used. These tests are done without outliers (outliers are treated).

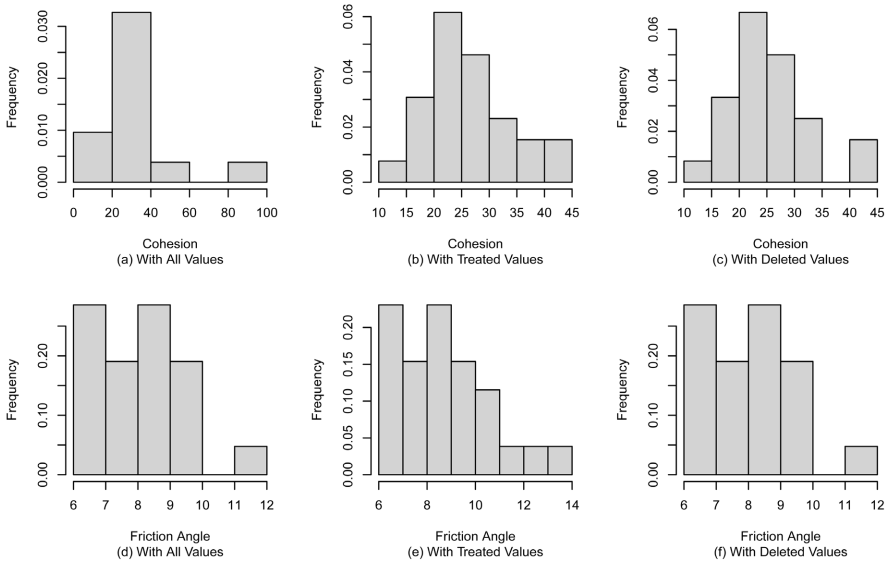

Figure 8. Histogram of cohesion and friction angle.

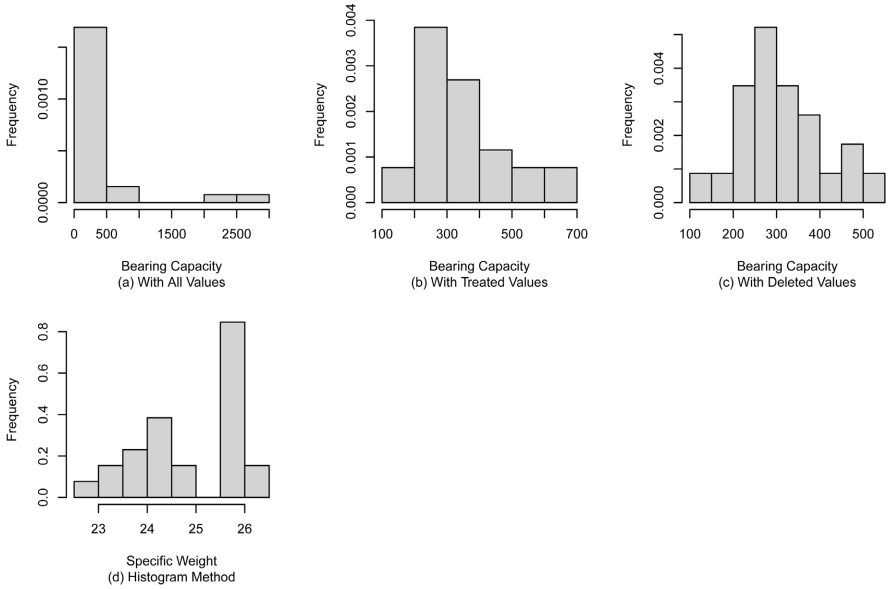

Figure 9. Histogram of bearing capacity and specific weight.

Table 8. Statistical indicators without outliers.

Cohesion (kPa)	Friction Angle φ (˚)	Specific gravity (kN/m^3)	Bearing Capacity Q_p (kPa)
26	26	26	26
10.12	6.15	22.83	149.4
44.76	13.55	26.36	652.5
26.39	8.83	24.91	348.6
8.46	1.94	1.07	137.95
0.320	0.22	0.04	0.4

- Graphical test

Figures 10(a)-(d) show that the probability distribution of the cohesion can be considered as Gaussian according to all these graphical methods.

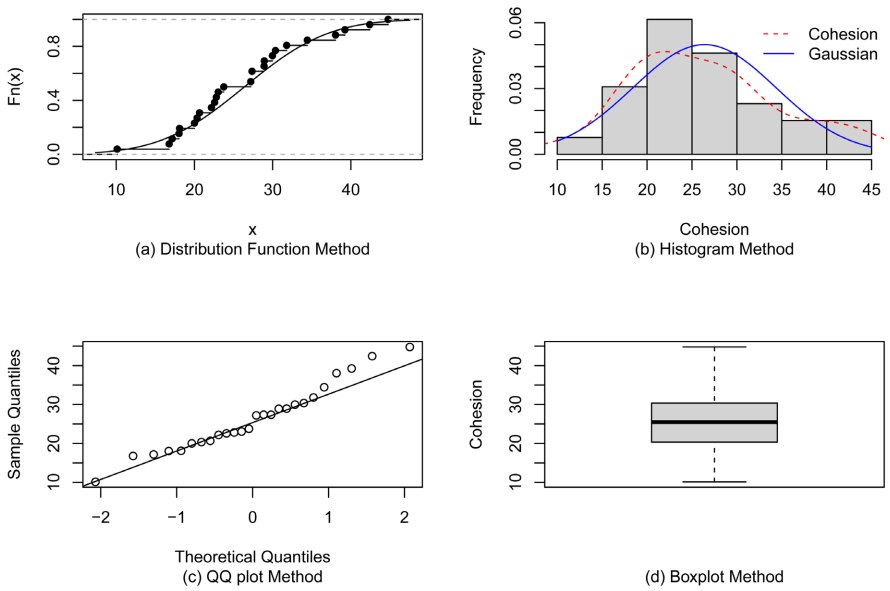

Figure 10. Graphical test for cohesion.

The same remark can be applied to Figures 11(a)-(d), which show that the probability distributions for the friction angle can be assimilated to the normal law. But with boxplot method (Figure 11(d)), on may say this distribution is not symmetrical.

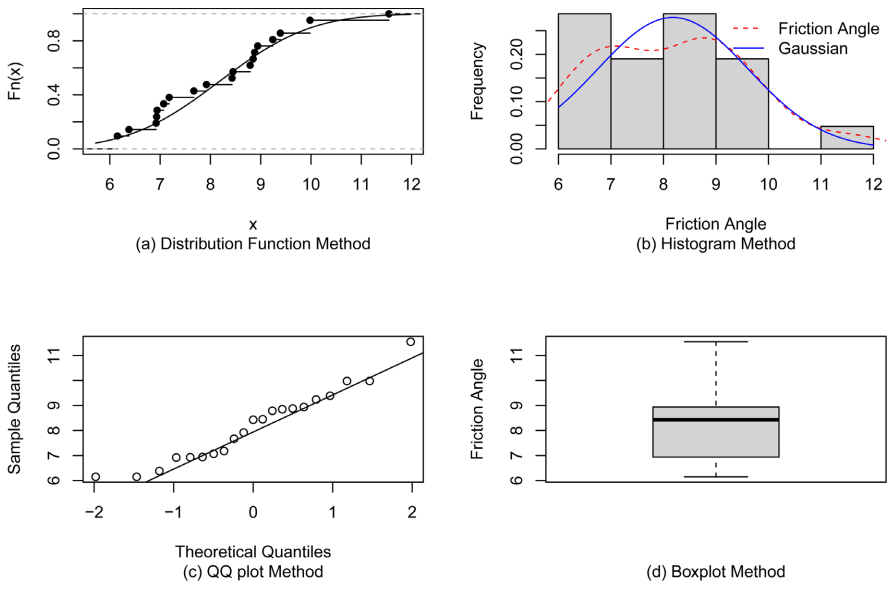

Figure 11. Graphical test for friction angle.

For Figures 12(a)-(d), we can also conclude that the probability laws for the

bearing capacity can be assimilated to the normal law.

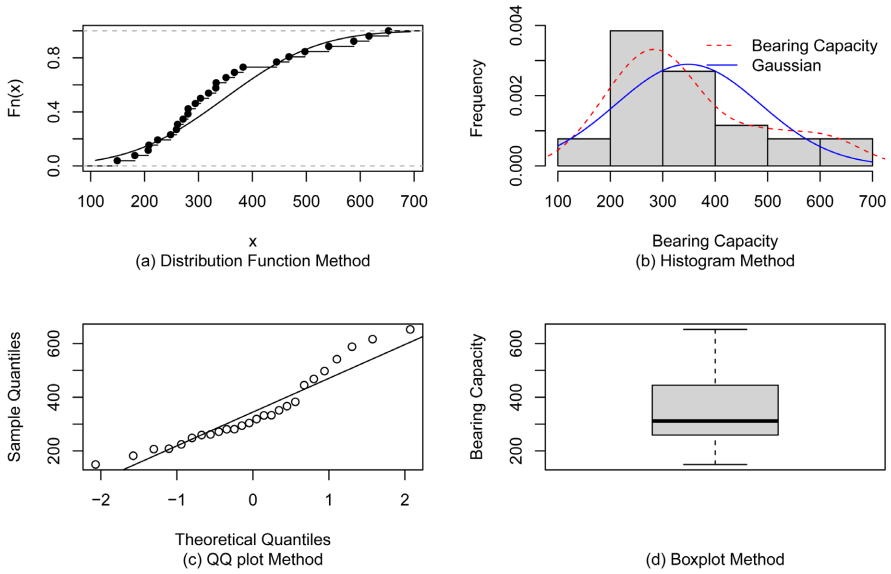

Figure 12. Graphical test for bearing capacity.

Regarding the specific weight, there is no outliers. The graphical test is shown in **Figure 13**. One can see the normal distribution could match with the probability distribution of the specific weight.

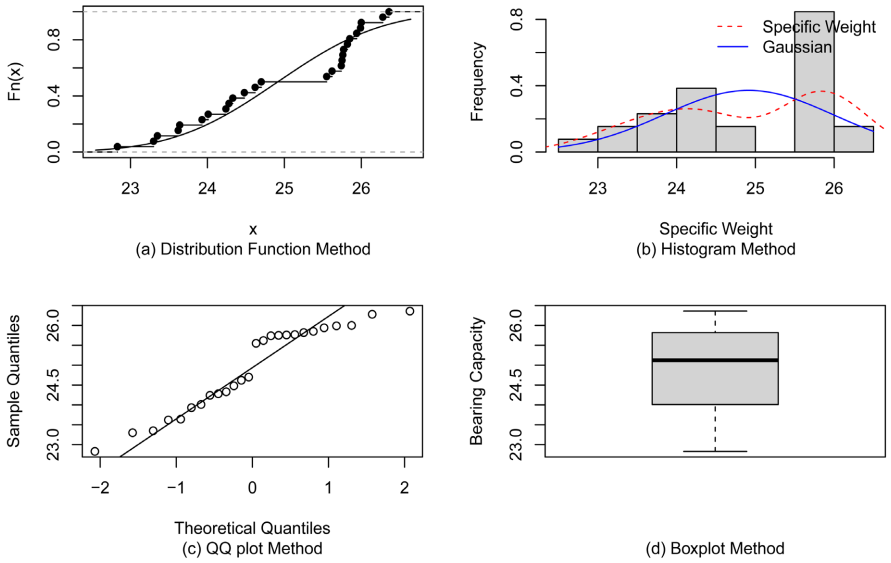

Figure 13. Graphical test for specific weight.

- Kolmogorov-Smirnov and Shapiro-Wilk tests

Table 9 shows the results of the probability distribution tests for treated values of the cohesion, the friction angle and the bearing capacity, and for non treated values of the specific weight by using RStudio Software. The normality H_0 hypothesis can not be rejected for the Kolmogorov test for the cohesion and the friction

angle and the specific weight, but for the bearing capacity it's rejected. However, it is important to notify that the p-value for normality distributions of the cohesion and the friction angle is high and close to 100% , that's meaning the H_0 hypothesis is close to be accepted. Whilst for the bearing capacity it's low. By doing the same test of normality with Shapiro-Wilk, one can conclude the same for the cohesion and the friction angle than the results of Kolmogorov test. But for the bearing capacity, its normality distributions are almost rejected. The lognormal distribution H_0 Hypothesis was also tested with the Kolmogorov-Smirnov method, one can conclude that the bearing capacity probability distribution matches with a lognormal distribution, whilst for the specific weigh, the friction angle the H_0 hypothesis is rejected. Also with a low probability of Kolmogorov test, the lognormal distribution can be used for the cohesion.

Table 9. Statistical tests results.

	Normal Distribution						Lognormal Distribution		
	Kolmogorov-Smirnov			Shapiro-Wilk			Kolmogorov-Smirnov		
Parameters	D	P-value	H_0	W	P-value	H_0	D	P-value	H_0
Cohesion (kPa)	0.123	0.828	Acc	0.965	0.511	Acc	0.195	0.275	Acc
Friction Angle (˚)	0.139	0.811	Acc	0.952	0.372	Acc	0.404	0.002	Rej
Bearing Capacity (kPa)	0.161	0.464	Rej	0.920	0.046	Rej	0.199	0.222	Acc
Specific Weight	0.223	0.127	Acc	0.903	0.02	Rej	0.5	1.5*10-6	Rej

Acc = Accepted, Rej = Rejected.

3.4. Discussions

This study was is done with a small sample size of 26. After outliers treatment of the geotechnical parameters, with a risk of 5%, the normal probability distribution was tested with Kolmogorow-Smirnov and Shapiro-Wilk methods. The presence of outliers causes a slight difference in the results of the calculation of geotechnical parameter uncertainties. However, the difference is more noticeable when determining the probability distribution that best fits the data. A goodness-of-fit test can give probability distributions that vary depending on the treatment of outliers.

4. Conclusion

At this stage, one can consider that with a good treatment, the probability distribution for the cohesion, the friction angle and the specific of Daral Peulh soil can be considered as normal distribution for probabilistic design. For the bearing capacity, the suitable probability distribution is the lognormal distribution. However, the probability distribution tests were done with a small sample number, it's necessary to do more laboratory tests for Daral Peulh site to confirm these results. It is also possible to conduct a correlation study. It is important to note that for the cohesion, the friction angle and the lognormal probability distribution can be

also used for design as quoted by some authors [11].

Conflicts of Interest

The authors declare no conflicts of interest regarding the publication of this paper.

References

[1] Lekehal, S. (2020) Evaluation de la Sécurité des Fondations Superficielles reposant sur des Sols Sableux à Paramètres Corrélés. Master's Thesis, Ecole Nationale Polytechnique.

[2] Doubbakh, R. (2020) Contribution à l'étude des fondations Superficielles par une approche Probabiliste. Ph.D. Thesis, Université Mohamed khider-Biskra.

[3] Magnan, J. (2000) Quelques spécificités du problème des incertitudes en géotechnique. *Revue Française de Géotechnique*, No. 93, 3-9. https://doi.org/10.1051/geotech/2000093003

[4] Abid, S. and Sakher, I. (2022) Apport de l'analyse statistique pour la caractérisation géotechnique des sols. Mémoire de Master, Université Larbi Tebessi-Tébessa.

[5] Baecher, G. (1987) Statistical Analysis of Geotechnical Data. Contract Report GL-87-1.

[6] Baziz, K. (2011) Effet de la variabilité des paramètres de calcul sur la stabilité des murs de soutènement. Ph.D. Thesis, Universite Mouloud Mammeri.

[7] Magnan, J.P. (1982) Les méthodes statistiques et probabilistes en mécanique des sols. Presse de l'ENPC France.

[8] Cassan, M. (2000) Utilisation de la statistique descriptive en géotechnique. *Revue Française de Géotechnique*, No. 93, 21-34. https://doi.org/10.1051/geotech/2000093021

[9] Chesneau, C. (2016) Introduction aux lois de probabilités avec R. Licence. France. Cel-01389942.

[10] Sanou, A. (2020) Analyse des données et des incertitudes sur les paramètres physiques et mécaniques de l'argile sensible dans la région du Saguenay-Lac-Saint-Jean. Ph.D. Thesis, Université du Québec à Chicoutimi.

[11] Bouhenniche, M.A., Massafer, T., Touzout, M.A. and Nechnech, A. (2019) Analyses probabilistes de stabilité des pentes—Étude de cas. *Rencontres Nationales de Génie Civil et d' Hydraulique*, Skikda, 13-14 Novembre 2019.